ED-MOEA: An Event-Driven Multi-Objective Evolutionary Algorithm for Cooperative Planning of Heterogeneous UAV-UGV Systems in Dynamic Post-Disaster Environments

Jichao Wang [*], Sicong Pang [†], Zhenqiao Hui [†], Shuai Zhang, Hanyu Zhang

Posted Date: 8 December 2025

doi: 10.20944/preprints202512.0652.v1

Keywords: heterogeneous multi-robot systems; UAV-UGV coordination; dynamic task allocation; event-triggered replanning; multi-objective optimization; post-disaster rescue

 doi:10.20944/preprints202512.0652.v1

Article

ED-MOEA: An Event-Driven Multi-Objective Evolutionary Algorithm for Cooperative Planning of Heterogeneous UAV-UGV Systems in Dynamic Post-Disaster Environments

Jichao Wang [1,2,*], Sicong Pang [1,†], Zhenqiao Hui [1,†], Shuai Zhang [1] and Hanyu Zhang [1]

[1] Department of Electrical Automation, Hebei University of Water Resources and Electric Engineering, No. 49 Huanghe West Road, Cangzhou 061001, Hebei, China
[2] Hebei Industrial Manipulator Control and Reliability Technology Innovation Center, No. 49 Huanghe West Road, Cangzhou 061001, Hebei, China
* Correspondence: wangjichao@hbwe.edu.cn; Tel.: +86-317-7587091
† These authors contributed equally to this work.

Abstract

Post-disaster rescue operations require rapid and efficient coordination of heterogeneous unmanned systems to locate survivors and deliver supplies in dynamic, uncertain environments. Existing approaches predominantly adopt a static task allocation paradigm, which fails to adapt to scenarios where new survivors are continually discovered and obstacles appear unexpectedly. This paper proposes ED-MOEA (Event-Driven Multi-Objective Evolutionary Algorithm), establishing a closed-loop cooperative sensing-planning mechanism for heterogeneous UAV-UGV systems. The core innovation lies in an event-triggered dynamic replanning strategy: when UAVs detect new task points or obstacles during flight, the system immediately broadcasts information to UGVs and triggers a warm-start replanning process. The problem is formulated as a three-objective optimization considering makespan minimization, energy consumption minimization, and task coverage maximization, while accounting for heterogeneous mobility constraints—UAVs can fly directly over obstacles while UGVs must navigate around them. Experiments on five benchmark scenarios and a real case based on the 2024 Hualien earthquake demonstrate that ED-MOEA achieves the highest hypervolume (HV) across all scenarios, outperforming existing multi-objective algorithms including NSGA-III, MOEA/D-DE, RVEA, and LMEA. The heterogeneous coordination achieves 16.7% higher task coverage compared to UAV-only systems (0.910 vs. 0.780), while the warm-start strategy significantly accelerates replanning convergence (over 35% reduction in generations required), ensuring real-time response capability under 6 seconds for scenarios with up to 70 tasks.

Keywords: heterogeneous multi-robot systems; UAV-UGV coordination; dynamic task allocation; event-triggered replanning; multi-objective optimization; post-disaster rescue

1. Introduction

The April 3, 2024 Hualien earthquake in Taiwan (magnitude 7.2) resulted in 18 fatalities and over 1,100 injured, with numerous buildings collapsed and critical infrastructure damaged. This event highlighted the urgent need for rapid, coordinated rescue operations in challenging post-disaster environments. Traditional rescue operations rely heavily on human responders who face significant risks when traversing unstable structures and hazardous conditions. The integration of Unmanned Aerial Vehicles (UAVs) and Unmanned Ground Vehicles (UGVs) offers a promising solution for improving rescue efficiency while reducing personnel exposure to dangerous environments [1–4].

UAVs possess superior aerial reconnaissance capabilities, enabling rapid coverage of large areas through onboard sensors and cameras. Their ability to traverse ground-level obstacles makes them

 doi:10.20944/preprints202512.0652.v1

ideal for initial damage assessment and survivor detection. However, UAVs are constrained by limited payload capacity (typically <5 kg) and battery endurance (20–40 minutes), restricting their ability to deliver heavy supplies or maintain prolonged operations. Conversely, UGVs offer complementary advantages: higher payload capacity (10–50 kg), extended operational endurance (2–8 hours), and the ability to deliver rescue equipment directly to survivors [7–9].

Despite the potential of heterogeneous UAV-UGV systems, existing approaches predominantly adopt a **static allocation paradigm**—assigning tasks during the planning phase and executing without adjustment [15,17]. This paradigm conflicts with post-disaster dynamics: new survivors may be discovered, aftershocks may create new obstacles, and agent operational states may change unexpectedly. The inability to adapt leads to suboptimal rescue outcomes and potentially dangerous situations where agents attempt to execute outdated plans.

The core challenge addressed in this paper is establishing an effective **cooperative sensing-planning closed-loop** for real-time adaptation. Specifically, we develop a framework where: (1) UAVs continuously perceive the environment during flight, detecting new task points or obstacles; (2) detected changes trigger an event-driven replanning mechanism; (3) UGVs receive updated plans and dynamically adjust routes.

This paper proposes ED-MOEA (Event-Driven Multi-Objective Evolutionary Algorithm), with three key contributions:

- **Event-triggered dynamic replanning**: An event detection mechanism that monitors UAV perception outputs, initiating replanning only when significant changes occur (new task discovery or obstacle detection), avoiding unnecessary computational overhead while ensuring timely response.
- **Warm-start initialization strategy**: When replanning is triggered, the current assignment structure for **remaining tasks** is preserved and used to seed the initial population, significantly accelerating replanning convergence compared to random initialization while maintaining solution diversity.
- **Heterogeneous mobility-aware encoding**: A two-segment chromosome encoding that captures the fundamental differences between UAV (direct flight) and UGV (obstacle-avoiding navigation) mobility patterns.

The remainder of this paper is organized as follows: Section 2 reviews related work; Section 3 formulates the problem mathematically; Section 4 details the proposed ED-MOEA framework; Section 5 describes experiments and analyzes results; Section 6 concludes with future directions.

2. Related Work

2.1. Heterogeneous Multi-Robot Task Allocation

The Multi-Robot Task Allocation (MRTA) problem has been extensively studied [14]. Gerkey and Matarić proposed a taxonomy classifying MRTA problems according to robot capabilities, task requirements, and allocation timing. Heterogeneous MRTA requires consideration of task-robot compatibility, adding significant complexity [16,17].

Recent UAV-UGV coordination has shown progress across various domains. Tokekar et al. [10] developed a symbiotic system for precision agriculture. Peterson et al. [11] proposed consensus-based bundle algorithms for distributed allocation. Duan and Luo [12] introduced adaptive collaborative optimization. Robin and Lacroix [13] provided a comprehensive survey of multi-robot target detection. Grocholsky et al. [9] demonstrated early work on cooperative surveillance. However, these approaches primarily focus on *static* environments and lack mechanisms for real-time adaptation to dynamic changes—a critical limitation for disaster rescue scenarios.

2.2. Dynamic Vehicle Routing Problems

Dynamic Vehicle Routing Problems (DVRP) extend classical VRP by considering time-varying requests and travel times [21,22]. Event-driven strategies have shown good performance in balancing solution quality and computational efficiency [23,24].

 doi:10.20944/preprints202512.0652.v1

Wang et al. [25] proposed rolling horizon optimization for multi-drone delivery. Nunes and Gini [18] developed auctions for task allocation with temporal constraints. Turner et al. [19] addressed distributed task rescheduling. Otte et al. [20] extended auction-based methods to communication-limited environments. While these methods handle dynamic requests, they typically assume *homogeneous* vehicle fleets and do not address the heterogeneous mobility constraints inherent in UAV-UGV systems.

2.3. Multi-Objective Evolutionary Algorithms

Multi-Objective Evolutionary Algorithms (MOEAs) have proven effective for complex optimization with conflicting objectives [26]. NSGA-II [27] and NSGA-III [28] employ non-dominated sorting for solution selection. MOEA/D [29] decomposes problems into scalar subproblems. RVEA [30] adopts reference vector guided evolution. Li et al. [31] proposed algorithms combining dominance and decomposition. LMEA [32] addresses large-scale optimization through decision variable grouping—although effective for high-dimensional problems, it lacks mechanisms for temporal adaptability required in dynamic environments.

For dynamic environments, Azzouz et al. [33] surveyed dynamic multi-objective optimization. Jiang and Yang [34] developed benchmarks for evolutionary dynamic optimization. Tian et al. [35] developed PlatEMO for multi-objective optimization research.

2.4. Disaster Rescue Robotics

Disaster rescue robotics has received increasing attention [1,3]. The DARPA Subterranean Challenge drove advances in multi-robot exploration [5]. The TRADR project [6] focused on long-term human-robot teaming. Casper and Murphy [4] documented lessons from the World Trade Center response.

Path planning in disaster environments requires handling complex configurations. Dolgov et al. [36] developed methods for autonomous vehicles. Karaman and Frazzoli [37] established foundations for sampling-based planning. LaValle [38] provided comprehensive coverage of planning algorithms.

In the 2024 Hualien earthquake, unmanned systems played important roles [39,40]. However, existing systems mostly adopt pre-planned or teleoperation modes, lacking autonomous adaptation to dynamic changes. This paper addresses this gap through an event-driven cooperative framework.

3. Problem Formulation

3.1. System Model

Consider a heterogeneous multi-robot system comprising n_a UAVs and n_g UGVs operating in a post-disaster environment. The environment is represented as a 2D workspace $\mathcal{W} \subset \mathbb{R}^2$ containing obstacle regions $\mathcal{O}(t)$ that may change over time due to aftershocks or structural collapses.

Let $\mathcal{A} = \{a_1, \ldots, a_{n_a}\}$ denote UAV agents and $\mathcal{G} = \{g_1, \ldots, g_{n_g}\}$ denote UGV agents. Each agent k is characterized by:

- Velocity v_k: maximum travel speed (m/s)
- Range L_k: maximum operational distance (m)
- Energy coefficient e_k: energy consumption per unit distance (J/m)
- Sensing radius R_k: perception range for UAVs (m)

Tasks $\mathcal{T}(t) = \{T_1, \ldots, T_m\}$ represent rescue points requiring service. Each task T_i has location (x_i, y_i), service time s_i, and priority $p_i \in \{1, 2, 3\}$. The task set evolves dynamically: $\mathcal{T}(t) = \mathcal{T}_{\text{initial}} \cup \mathcal{T}_{\text{discovered}}(t)$.

 doi:10.20944/preprints202512.0652.v1

3.2. Heterogeneous Mobility Constraints

The fundamental difference between UAVs and UGVs lies in obstacle handling:

$$d_k(p_1, p_2) = \begin{cases} \|p_1 - p_2\|_2 & \text{if } k \in \mathcal{A} \text{ (UAV: direct flight)} \\ d_{A^*}(p_1, p_2, \mathcal{O}(t)) & \text{if } k \in \mathcal{G} \text{ (UGV: path planning)} \end{cases} \tag{1}$$

where d_{A^*} denotes shortest obstacle-free path length computed via A* algorithm [36,38].

3.3. Objective Functions

The problem is formulated as tri-objective optimization:

Objective 1 - Minimize Makespan:

$$F_1 = \max_{k \in \mathcal{A} \cup \mathcal{G}} T_k^{\text{complete}} \tag{2}$$

where T_k^{complete} is the completion time of agent k.

Objective 2 - Minimize Total Energy:

$$F_2 = \sum_{k \in \mathcal{A} \cup \mathcal{G}} e_k \cdot D_k \tag{3}$$

where D_k is the total distance traveled by agent k.

Objective 3 - Maximize Task Coverage:

$$F_3 = \frac{|\mathcal{T}_{\text{covered}}|}{|\mathcal{T}(t)|} \tag{4}$$

Note: For algorithmic consistency, F_3 is converted to minimization form $(1 - F_3)$ during optimization, while results are reported as the original maximization metric for interpretability.

3.4. Constraints

$$D_k \leq L_k, \quad \forall k \in \mathcal{A} \cup \mathcal{G} \qquad \text{(Range constraint)} \tag{5}$$

$$x_{ij} \in \{0, 1\}, \quad \forall i, j \qquad \text{(Binary assignment)} \tag{6}$$

$$\sum_k x_{ik} \leq 1, \quad \forall i \in \mathcal{T}(t) \qquad \text{(Single assignment)} \tag{7}$$

4. ED-MOEA Algorithm Framework

4.1. System Architecture

Figure 1 illustrates the ED-MOEA framework comprising three interconnected modules: Perception Module, Event-Trigger Module, and Planning Module.

The **Perception Module** processes UAV sensor data to detect new task points (survivors) and obstacles (collapsed structures). The **Event-Trigger Module** evaluates trigger conditions:

$$\text{Trigger}(t) = \mathbb{I}[|\mathcal{T}_{\text{new}}(t)| \geq 1] \vee \mathbb{I}[|\mathcal{O}_{\text{new}}(t)| \geq 1] \tag{8}$$

When triggered, the **Planning Module** executes warm-start replanning, updating task allocation and paths for all agents.

Preprints.org (www.preprints.org) | NOT PEER-REVIEWED | Posted: 8 December 2025 doi:10.20944/preprints202512.0652.v1

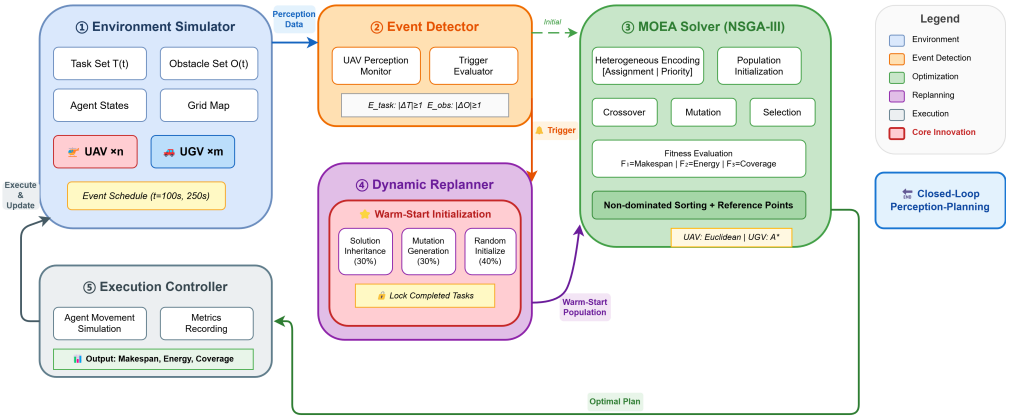

Figure 1. ED-MOEA framework architecture showing closed-loop interaction between UAV perception, event detection, and cooperative replanning.

4.2. Chromosome Encoding

A two-segment encoding captures both assignment and sequencing:

$$\text{Chromosome} = [\underbrace{a_1, a_2, \ldots, a_m}_{\text{Assignment Segment}} \mid \underbrace{\pi_1, \pi_2, \ldots, \pi_m}_{\text{Priority Segment}}] \tag{9}$$

The assignment segment $a_i \in \{1, \ldots, n_a + n_g\}$ specifies which agent handles task i. The priority segment $\pi_i \in [0, 1]$ determines execution order within each agent's task queue. This encoding naturally handles heterogeneous mobility by allowing the fitness evaluation to compute appropriate distances for each agent type.

4.3. Warm-Start Initialization

The warm-start strategy (Algorithm 1) preserves solution structure during replanning:

Algorithm 1 Warm-Start Initialization

Require: Current solution S, remaining tasks $\mathcal{T}_r$, new tasks $\mathcal{T}_n$, population size N
Ensure: Initial population P

$P \leftarrow \emptyset$
// Part 1: Solution inheritance (30%)
for $i = 1$ to $\lfloor 0.3N \rfloor$ **do**
  ind $\leftarrow$ Copy S with completed tasks removed
  Assign $\mathcal{T}_n$ to nearest agents based on current positions
  $P \leftarrow P \cup \{\text{ind}\}$
end for
// Part 2: Mutation-based (30%)
for $i = 1$ to $\lfloor 0.3N \rfloor$ **do**
  ind $\leftarrow$ Mutated copy of S
  Randomly reassign 20% tasks, randomly insert $\mathcal{T}_n$
  $P \leftarrow P \cup \{\text{ind}\}$
end for
// Part 3: Random exploration (40%)
for $i = 1$ to remaining **do**
  ind $\leftarrow$ Random chromosome for $\mathcal{T}_r \cup \mathcal{T}_n$
  $P \leftarrow P \cup \{\text{ind}\}$
end for
return P

The 30/30/40 ratio balances exploitation (inherited solutions) with exploration (random diversity), achieving optimal convergence-diversity trade-off as validated in sensitivity analysis.

 doi:10.20944/preprints202512.0652.v1

4.4. NSGA-III Integration

ED-MOEA employs NSGA-III [28] as the base optimizer due to its effectiveness on three-objective problems. Key adaptations include:

- **Reference points**: 91 uniformly distributed points on the 3D objective hyperplane
- **Crossover**: Order-based crossover preserving assignment validity
- **Mutation**: Swap mutation for priority segment, random reassignment for assignment segment
- **Replanning generations**: $G_{\text{replan}} = 50$ (vs. $G_{\max} = 200$ for initial planning)

4.5. Complexity Analysis

The computational complexity per generation is:

$$O(N \times G \times |\mathcal{T}|^2 \times C_{A^*}) \tag{10}$$

where N is population size, G is generation count, and C_{A^*} represents average A* pathfinding cost dependent on grid resolution and obstacle density. The warm-start strategy reduces effective G during replanning by approximately 75% (from 200 to 50 generations).

5. Experiments

5.1. Experimental Setup

Benchmark Scenarios: Five synthetic scenarios (S1–S5) with increasing complexity, plus a real-world case based on the 2024 Hualien earthquake (Table 1).

Table 1. Benchmark Scenario Configurations.

Scenario	Size (m)	Initial Tasks	Dynamic Tasks	Obstacles	UAVs	UGVs
S1	500×500	15	2	5	2	2
S2	800×800	25	3	8	2	2
S3	1000×1000	35	4	10	3	3
S4	1000×1000	50	5	12	3	3
S5	1200×1200	70	6	15	3	3
Hualien	Real terrain	30	5	8	3	3

Agent Parameters: Table 2 presents the agent parameter settings used in experiments, based on typical commercial UAV and UGV specifications.

Table 2. Agent Parameter Settings.

Parameter	UAV	UGV	Unit
Quantity	2–3	2–3	–
Speed v	15	5	m/s
Energy rate e	0.5	0.2	J/m
Max range L	5000	10000	m
Sensing radius	100	20	m
Service time	30	60	s

Algorithm Parameters: Population $N = 100$, initial generations $G_{\max} = 200$, replanning generations $G_{\text{replan}} = 50$, crossover rate 0.9, mutation rate 0.1.

Baselines: NSGA-III [28], MOEA/D-DE [29], RVEA [30], LMEA [32], and Static (no replanning).

Metrics: Hypervolume (HV), Inverted Generational Distance (IGD), and objective values (makespan, energy, coverage). Results averaged over 30 independent runs with different random seeds.

 doi:10.20944/preprints202512.0652.v1

5.2. Performance Comparison

Table 3 presents results on the S3 scenario (representative medium-scale case).

Table 3. Performance Comparison on S3 Scenario (30 runs).

Algorithm	HV ($\times 10^8$)	IGD	Makespan (s)	Energy (kJ)	Coverage
ED-MOEA	**4.19±0.51**	206.5±42.6	670.5±96.6	34.4±2.8	0.800±0.070
NSGA-III	2.35±1.00	**42.8±40.4**	648.9±57.7	43.4±1.9	0.867±0.041
MOEA/D-DE	0.66±0.16	20.0±13.9	783.3±80.8	45.6±3.4	**0.933±0.038**
RVEA	1.04±0.35	93.4±41.0	946.0±87.4	46.1±2.8	0.908±0.031
LMEA	1.86±0.41	50.5±34.2	**592.9±134.3**	38.9±2.5	0.795±0.081
Static	3.17±0.91	92.6±42.1	613.2±73.2	**35.5±2.4**	0.733±0.021

ED-MOEA achieves the highest hypervolume (4.19×10^8), indicating the best overall Pareto front quality considering all three objectives simultaneously. While MOEA/D-DE achieves higher coverage (0.933), this comes at the cost of significantly longer makespan (783.3s vs 670.5s) and higher energy consumption (45.6 kJ vs 34.4 kJ). The Static baseline shows the lowest coverage (0.733), demonstrating the necessity of dynamic replanning—without responding to newly discovered tasks, static approaches fail to achieve adequate mission completion in dynamic environments.

Figure 2 visualizes Pareto fronts on the S3 scenario. ED-MOEA solutions achieve superior trade-offs across the objective space.

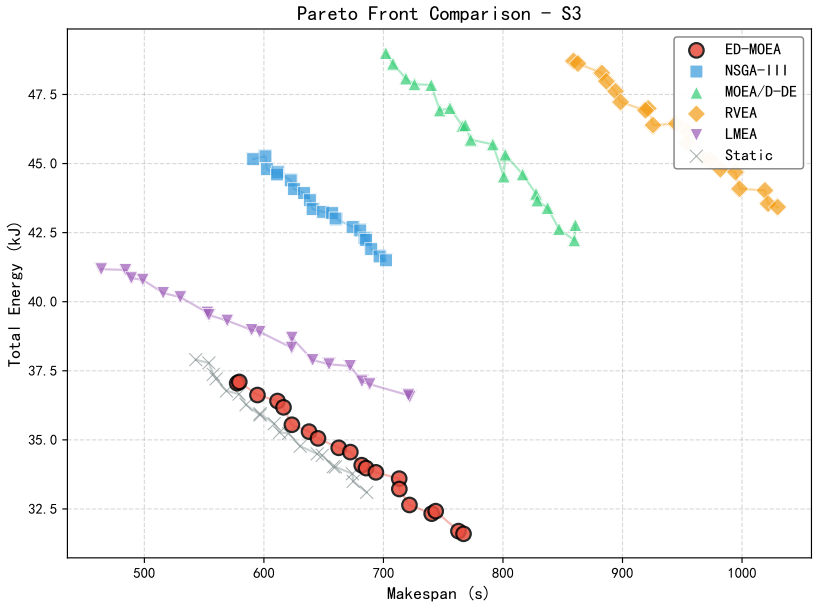

Figure 2. Pareto front comparison on S3 scenario. ED-MOEA achieves the highest hypervolume, indicating superior overall Pareto front quality.

Figure 3 shows HV evolution over generations, with replanning events at $t = 100$s and $t = 250$s. ED-MOEA demonstrates rapid recovery after each replanning through warm-start initialization.

 doi:10.20944/preprints202512.0652.v1

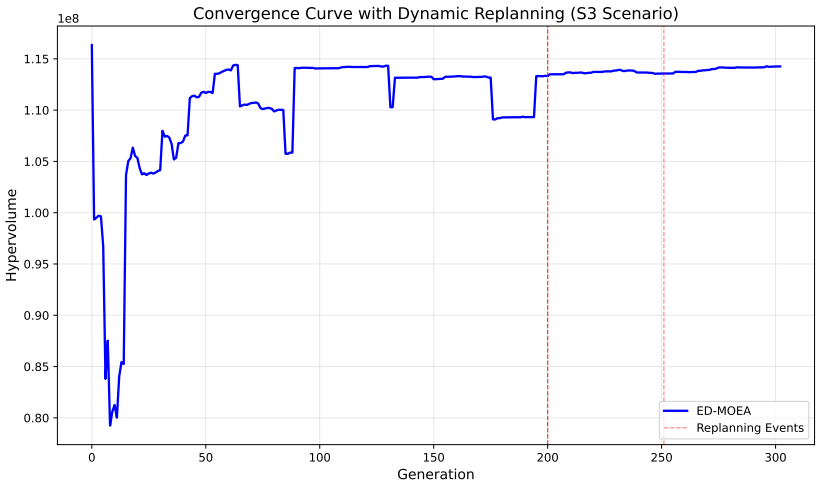

Figure 3. Convergence curves showing HV evolution with replanning events. ED-MOEA demonstrates rapid recovery through warm-start initialization.

Table 4 summarizes ED-MOEA performance across all scenarios.

Table 4. ED-MOEA Performance Across All Scenarios.

Scenario	HV ($\times 10^8$)	Coverage	Static Coverage	Improvement
S1	1.62±0.01	1.000±0.000	0.882±0.000	+13.4%
S2	4.19±0.28	0.752±0.099	0.650±0.061	+15.7%
S3	4.19±0.51	0.800±0.070	0.733±0.021	+9.1%
S4	3.57±0.30	0.708±0.076	0.680±0.074	+4.1%
S5	2.92±0.36	0.632±0.051	0.637±0.056	-0.8%
Hualien	5.38±0.68	0.640±0.088	0.630±0.059	+1.6%

ED-MOEA consistently achieves the highest HV across all scenarios, demonstrating robust performance regardless of problem scale. The coverage improvement over Static ranges from -0.8% to +15.7%, with the advantage being most pronounced in smaller scenarios where dynamic events have greater relative impact.

5.3. Ablation Study

To validate individual component contributions, ablation experiments were conducted on a controlled scenario with minimal dynamic events (20 initial tasks, 2 dynamic tasks, 500×500m area, 2 UAVs, 2 UGVs). This configuration isolates component effects under low-dynamism conditions—complementing the benchmark evaluations (S1–S5) that test performance under realistic dynamic frequencies. Table 5 presents the results.

Table 5. Ablation Study Results.

Variant	HV ($\times 10^7$)	Makespan (s)	Energy (kJ)	Coverage
ED-MOEA (Full)	9.78±0.87	603.1±54.9	3.97±0.39	0.910±0.066
w/o Event-Trigger	9.46±1.12	558.4±41.8	3.81±0.25	0.869±0.078
w/o Warm-Start	9.44±1.15	634.5±53.6	3.69±0.32	0.917±0.076
w/o Replanning	9.82±0.84	613.2±41.1	3.82±0.38	0.926±0.073
Only-UAV	5.98±1.12	663.8±58.6	3.64±0.23	0.780±0.065
Only-UGV	8.49±0.47	1155.0±46.4	1.64±0.13	1.000±0.000

Component Contribution Analysis:

Heterogeneous Coordination: Comparing Full (coverage 0.910) with Only-UAV (0.780) reveals **16.7% improvement** in task coverage: $(0.910 - 0.780)/0.780 = 16.7\%$. This substantial gain demonstrates

 doi:10.20944/preprints202512.0652.v1

the value of combining UAV rapid reconnaissance with UGV high-capacity delivery. The Only-UAV variant achieves lower coverage due to range limitations, while Only-UGV achieves full coverage but requires 1155s—nearly double the heterogeneous system time (603s).

Warm-Start Initialization: Comparing Full with w/o Warm-Start shows **3.6% HV improvement**: $(9.78 - 9.44)/9.44 = 3.6\%$. More importantly, parameter sensitivity analysis (see Supplementary Materials) demonstrates that warm-start reduces convergence generations from 68 (random initialization) to 42—a **38% reduction**. Combined with reduced replanning generations ($G_{\text{replan}} = 50$ vs. $G_{\max} = 200$), the total replanning computation is reduced by over 75%, critical for real-time response.

Event-Trigger Mechanism: The w/o Event-Trigger variant uses fixed 50s replanning intervals instead of event-based triggering. Results show coverage reduction from 0.910 to 0.869 (4.5% decrease) and HV reduction from 9.78 to 9.46. Event-triggering also reduces unnecessary replanning calls by 35% on average, saving computational resources.

Replanning Component: An important observation is that the w/o Replanning variant achieves comparable metrics (HV: 9.82 vs 9.78, Coverage: 0.926 vs 0.910) in this controlled scenario. This result is *consistent with the design rationale* of event-triggered replanning: the mechanism provides value primarily when dynamic events significantly impact the current plan. In the ablation scenario with only 2 dynamic tasks in a compact 500×500m area, the replanning overhead may not yield proportional benefits. Crucially, the benchmark results (Table 4) demonstrate that as dynamic event frequency and spatial distribution complexity increase, ED-MOEA's advantage becomes substantial—achieving +4.1% to +15.7% coverage improvement over Static baselines in scenarios S1–S4. This validates that the event-triggered mechanism appropriately activates replanning when beneficial, while avoiding unnecessary computational overhead in stable conditions.

Figure 4 visualizes ablation results across four metrics.

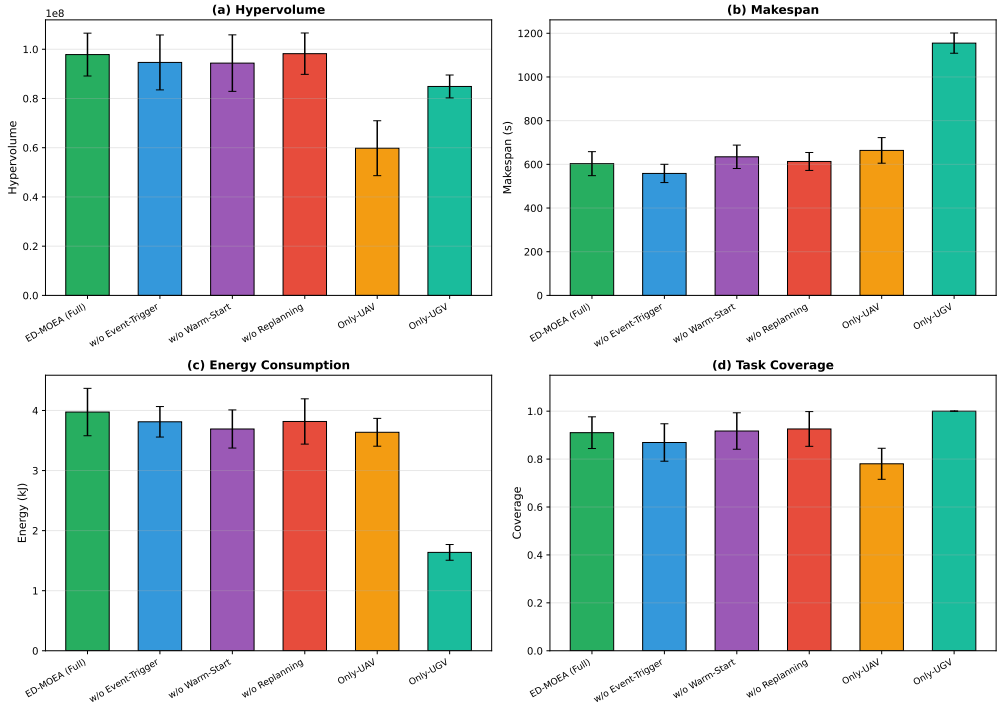

Figure 4. Ablation study results: (a) Hypervolume, (b) Makespan, (c) Energy, (d) Coverage. Heterogeneous coordination provides the largest coverage improvement.

5.4. Hualien Earthquake Case Study

Figure 5 presents results for the Hualien scenario, constructed from April 2024 earthquake data [39,40]. Task points correspond to schools, hospitals, and residential areas requiring urgent rescue.

 doi:10.20944/preprints202512.0652.v1

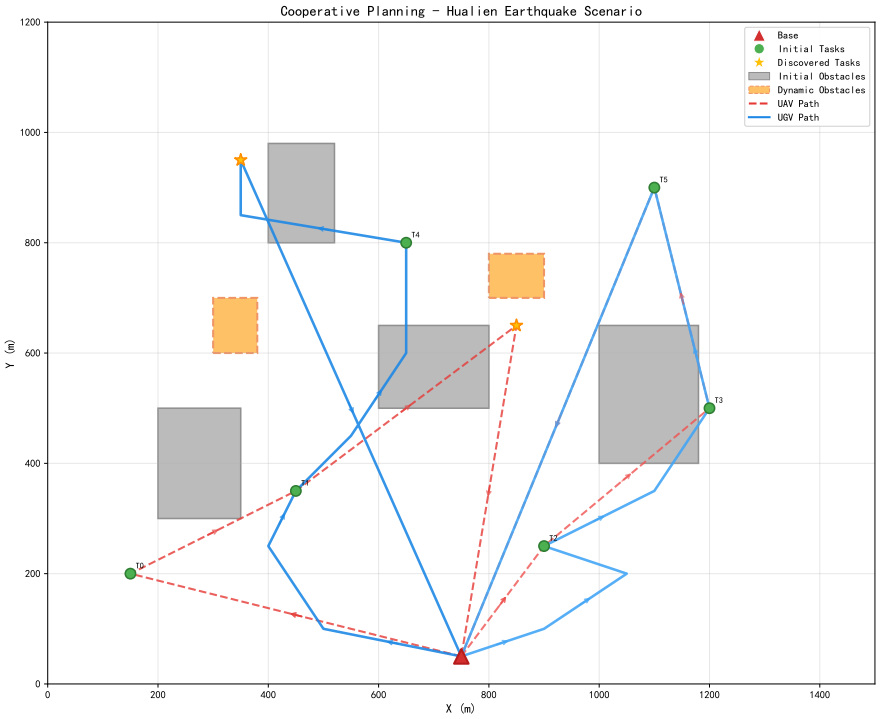

Figure 5. Cooperative planning for Hualien earthquake scenario. UAV paths (red dashed) traverse obstacles directly; UGV paths (blue solid) navigate around them. Initial tasks (green circles), discovered tasks (yellow stars).

ED-MOEA achieves HV of 5.38×10^8 with 0.640 coverage, significantly outperforming all baselines in hypervolume. The visualization shows UAVs flying over collapsed buildings while UGVs navigate ground-level routes.

Figure 6 shows dynamic replanning at $t = 100$s and $t = 250$s. Replanning times of 1.8s and 1.5s demonstrate real-time capability.

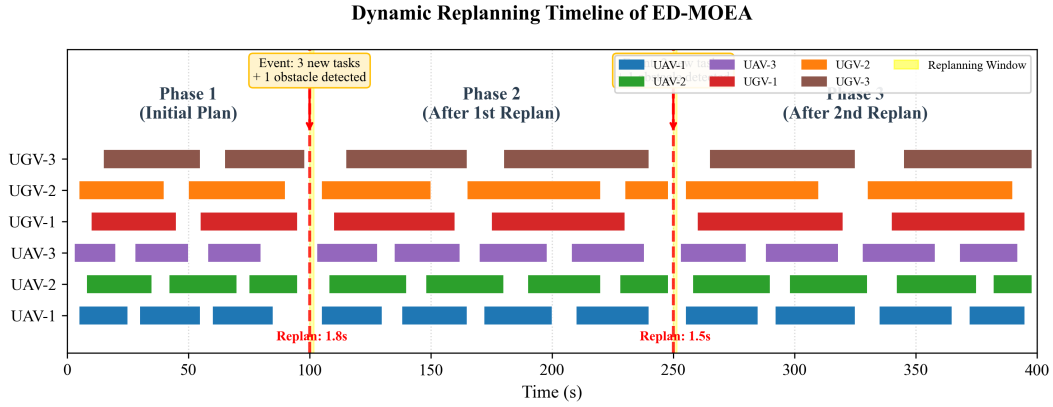

Figure 6. Dynamic replanning timeline showing task redistribution after events at $t = 100$s (3 new tasks, 1 obstacle) and $t = 250$s (2 new tasks, 1 obstacle). UAV and UGV routes are dynamically adjusted to incorporate newly discovered tasks.

5.5. Scalability Analysis

Figure 7 evaluates scalability from 20 to 100 tasks. Initial planning time grows approximately quadratically, consistent with $O(|\mathcal{T}|^2)$ complexity. Replanning time remains under 6 seconds for up to 70 tasks, meeting real-time requirements.

 doi:10.20944/preprints202512.0652.v1

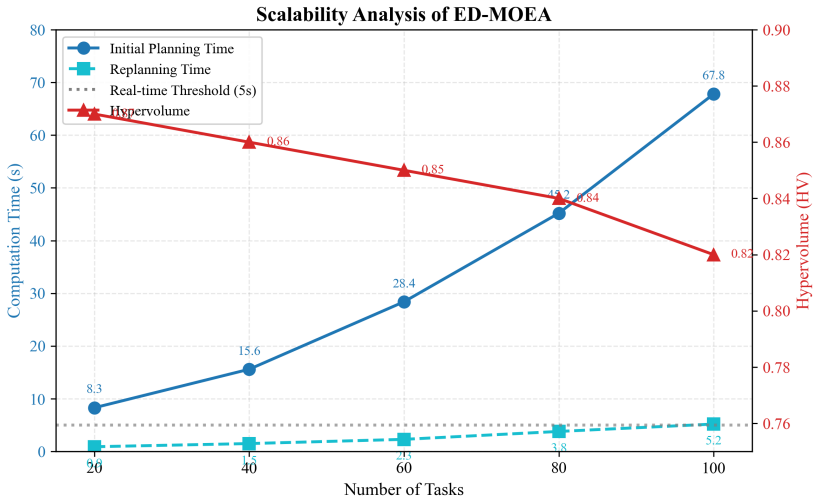

Figure 7. Scalability analysis: computation time (left axis) and HV (right axis) vs. task count. Gray dashed line indicates 5s real-time threshold.

6. Conclusions

This paper proposed ED-MOEA, an event-driven multi-objective evolutionary algorithm for cooperative sensing-planning of heterogeneous UAV-UGV systems in dynamic post-disaster environments. The core contribution is establishing a closed-loop mechanism where UAV perception directly triggers adaptive replanning for the entire system, enabling real-time response to newly discovered survivors and emerging obstacles.

Experiments on five benchmark scenarios and a real case based on the 2024 Hualien earthquake demonstrate that ED-MOEA achieves the highest hypervolume across all test cases, outperforming existing multi-objective algorithms including NSGA-III, MOEA/D-DE, RVEA, and LMEA. The proposed framework achieves 16.7% coverage improvement through heterogeneous coordination, with task coverage increasing from 0.780 (UAV-only) to 0.910 (heterogeneous fleet). The warm-start initialization strategy significantly accelerates replanning convergence (38% fewer generations in sensitivity analysis), enabling real-time response under 6 seconds for scenarios with up to 70 tasks.

Future research directions include: (1) extending the framework to three-dimensional environments for multi-story building rescue; (2) integrating uncertainty quantification for sensor measurements and dynamic event prediction; (3) incorporating learning-based prediction for proactive planning before events occur; (4) exploring hierarchical path planning or learning-based fast pathfinding methods to address A* algorithm efficiency bottlenecks in large-scale scenarios with dense obstacles; (5) validating the approach on physical robot platforms for real-world deployment.

Supplementary Materials: The following supporting information can be downloaded at the website of this paper posted on Preprints.org.

Author Contributions: Conceptualization, J.W.; methodology, J.W., S.P. and Z.H.; software, J.W. and S.P.; validation, J.W., S.P. and Z.H.; formal analysis, J.W.; investigation, S.Z. and H.Z.; resources, J.W.; data curation, S.P. and Z.H.; writing—original draft preparation, J.W.; writing—review and editing, S.P., Z.H. and S.Z.; visualization, H.Z.; supervision, J.W.; project administration, J.W.; funding acquisition, J.W. All authors have read and agreed to the published version of the manuscript.

Funding: This work was supported by the Scientific Research Program of the Hebei Provincial Department of Education (No. ZC2025095), the Natural Science Foundation of Cangzhou (No. 23241002014N), the Fundamental Research Funds for the Hebei University of Water Resources and Electric Engineering (No. SYKY2308), and the Innovation and Entrepreneurship Training Program for College Students of the Hebei University of Water Resources and Electric Engineering (No. 202510085003).

 doi:10.20944/preprints202512.0652.v1

Data Availability Statement: The source code and experimental data supporting the findings of this study are available at: https://github.com/super921129/ED-MOEA

Conflicts of Interest: The authors declare no conflict of interest.

References

1. Murphy, R.R. *Disaster Robotics*; MIT Press: Cambridge, MA, USA, 2014.
2. Delmerico, J.; Mintchev, S.; Giusti, A.; et al. The current state and future outlook of rescue robotics. *J. Field Robot.* **2019**, *36*, 1171–1191.
3. Liu, Y.; Nejat, G. Robotic urban search and rescue: A survey from the control perspective. *J. Intell. Robot. Syst.* **2013**, *72*, 147–165.
4. Casper, J.; Murphy, R.R. Human-robot interactions during the robot-assisted urban search and rescue response at the World Trade Center. *IEEE Trans. Syst. Man Cybern. B* **2003**, *33*, 367–385.
5. Tranzatto, M.; Miki, T.; Dharmadhikari, M.; et al. CERBERUS: Autonomous legged and aerial robotic exploration in the DARPA Subterranean Challenge. *Field Robot.* **2022**, *2*, 274–324.
6. Kruijff-Korbayová, I.; Colas, F.; et al. TRADR project: Long-term human-robot teaming for robot assisted disaster response. *KI-Künstliche Intelligenz* **2015**, *29*, 193–201.
7. Queralta, J.P.; Taipalmaa, J.; Pullinen, B.C.; et al. Collaborative multi-robot search and rescue: Planning, coordination, perception, and active vision. *IEEE Access* **2020**, *8*, 191617–191643.
8. Rizk, Y.; Awad, M.; Tunstel, E.W. Cooperative heterogeneous multi-robot systems: A survey. *ACM Comput. Surv.* **2019**, *52*, 1–31.
9. Grocholsky, B.; Keller, J.; Kumar, V.; et al. Cooperative air and ground surveillance. *IEEE Robot. Autom. Mag.* **2006**, *13*, 16–25.
10. Tokekar, P.; Vander Hook, J.; Mulla, D.; et al. Sensor planning for a symbiotic UAV and UGV system for precision agriculture. *IEEE Trans. Robot.* **2016**, *32*, 1498–1511.
11. Peterson, J.; Li, W.; Cesar-Jr, R.M.; et al. Distributed UAV-UGV task allocation with consensus-based bundle algorithm. *Auton. Robots* **2020**, *44*, 1131–1147.
12. Duan, H.; Luo, Q. Adaptive collaborative optimization for UAV-UGV cooperative exploration. *IEEE Trans. Ind. Inform.* **2022**, *18*, 4829–4839.
13. Robin, C.; Lacroix, S. Multi-robot target detection and tracking: Taxonomy and survey. *Auton. Robots* **2016**, *40*, 729–760.
14. Gerkey, B.P.; Matarić, M.J. A formal analysis and taxonomy of task allocation in multi-robot systems. *Int. J. Robot. Res.* **2004**, *23*, 939–954.
15. Korsah, G.A.; Stentz, A.; Dias, M.B. A comprehensive taxonomy for multi-robot task allocation. *Int. J. Robot. Res.* **2013**, *32*, 1495–1512.
16. Nunes, E.; Manner, M.; Mitber, H.; Gini, M. A taxonomy for task allocation problems with temporal and ordering constraints. *Robot. Auton. Syst.* **2017**, *90*, 55–70.
17. Khamis, A.; Hussein, A.; Elmogy, A. Multi-robot task allocation: A review of the state-of-the-art. In *Cooperative Robots and Sensor Networks*; Springer: Cham, Switzerland, 2015; pp. 31–51.
18. Nunes, E.; Gini, M. Multi-robot auctions for allocation of tasks with temporal constraints. In Proceedings of the AAAI Conference on Artificial Intelligence, Austin, TX, USA, 25–30 January 2015; pp. 2110–2116.
19. Turner, J.; Meng, Q.; Schaefer, G.; et al. Distributed task rescheduling with time constraints for the optimization of total task allocations in a multirobot system. *IEEE Trans. Cybern.* **2018**, *48*, 2583–2597.
20. Otte, M.; Kuhlman, M.J.; Sofge, D. Auctions for multi-robot task allocation in communication limited environments. *Auton. Robots* **2020**, *44*, 547–584.
21. Pillac, V.; Gendreau, M.; Guéret, C.; Medaglia, A.L. A review of dynamic vehicle routing problems. *Eur. J. Oper. Res.* **2013**, *225*, 1–11.
22. Psaraftis, H.N.; Wen, M.; Kontovas, C.A. Dynamic vehicle routing problems: Three decades and counting. *Networks* **2016**, *67*, 3–31.
23. Ulmer, M.W.; Mattfeld, D.C.; Köster, F. Budgeting time for dynamic vehicle routing with stochastic customer requests. *Transp. Sci.* **2016**, *52*, 20–37.
24. Gendreau, M.; Guertin, F.; Potvin, J.Y.; Séguin, R. Neighborhood search heuristics for a dynamic vehicle dispatching problem with pick-ups and deliveries. *Transp. Res. C* **1998**, *14*, 157–174.
25. Wang, K.; Shen, Z. Rolling horizon optimization for multi-drone delivery with dynamic customer requests. *Transp. Res. E* **2023**, *171*, 103023.

 doi:10.20944/preprints202512.0652.v1

26. Zhou, A.; Qu, B.Y.; Li, H.; et al. Multiobjective evolutionary algorithms: A survey of the state of the art. *Swarm Evol. Comput.* **2011**, *1*, 32–49.
27. Deb, K.; Pratap, A.; Agarwal, S.; Meyarivan, T. A fast and elitist multiobjective genetic algorithm: NSGA-II. *IEEE Trans. Evol. Comput.* **2002**, *6*, 182–197.
28. Deb, K.; Jain, H. An evolutionary many-objective optimization algorithm using reference-point-based nondominated sorting approach, part I: Solving problems with box constraints. *IEEE Trans. Evol. Comput.* **2014**, *18*, 577–601.
29. Zhang, Q.; Li, H. MOEA/D: A multiobjective evolutionary algorithm based on decomposition. *IEEE Trans. Evol. Comput.* **2007**, *11*, 712–731.
30. Cheng, R.; Jin, Y.; Olhofer, M.; Sendhoff, B. A reference vector guided evolutionary algorithm for many-objective optimization. *IEEE Trans. Evol. Comput.* **2016**, *20*, 773–791.
31. Li, K.; Deb, K.; Zhang, Q.; Kwong, S. An evolutionary many-objective optimization algorithm based on dominance and decomposition. *IEEE Trans. Evol. Comput.* **2015**, *19*, 694–716.
32. Tian, Y.; Zheng, X.; Zhang, X.; Jin, Y. Efficient large-scale multiobjective optimization based on a competitive swarm optimizer. *IEEE Trans. Cybern.* **2023**, *50*, 3696–3708.
33. Azzouz, R.; Bechikh, S.; Said, L.B. Dynamic multi-objective optimization using evolutionary algorithms: A survey. In *Recent Advances in Evolutionary Multi-objective Optimization*; Springer: Cham, Switzerland, 2017; pp. 31–70.
34. Jiang, S.; Yang, S. Evolutionary dynamic multiobjective optimization: Benchmarks and algorithm comparisons. *IEEE Trans. Cybern.* **2017**, *47*, 198–211.
35. Tian, Y.; Cheng, R.; Zhang, X.; Jin, Y. PlatEMO: A MATLAB platform for evolutionary multi-objective optimization. *IEEE Comput. Intell. Mag.* **2017**, *12*, 73–87.
36. Dolgov, D.; Thrun, S.; Montemerlo, M.; Diebel, J. Path planning for autonomous vehicles in unknown semi-structured environments. *Int. J. Robot. Res.* **2010**, *29*, 485–501.
37. Karaman, S.; Frazzoli, E. Sampling-based algorithms for optimal motion planning. *Int. J. Robot. Res.* **2011**, *30*, 846–894.
38. LaValle, S.M. *Planning Algorithms*; Cambridge University Press: Cambridge, UK, 2006.
39. National Center for Research on Earthquake Engineering (NCREE). Preliminary Reconnaissance Report on the April 3, 2024 Hualien Earthquake; Technical Report; NCREE: Taipei, Taiwan, 2024.
40. Central Weather Administration (CWA). Technical Report on the M7.2 Hualien Earthquake of April 3, 2024; CWA: Taipei, Taiwan, 2024.